Multiplicity dependence of freezeout scenarios in pp collisions at $\sqrt{s} = 7$ TeV

Susil Kumar Panda,[1,*] Sandeep Chatterjee,[2,†] Ajay Kumar Dash,[3,‡] Bedangadas Mohanty,[4,§] Rita Paikaray,[1,‖] Subhasis Samanta,[5,¶] and Ranbir Singh[4,#]

[1]*Department of Physics, Ravenshaw University, Cuttack - 753003, India*
[2]*Department of Physical Sciences, Indian Institute of Science Education and Research, Berhampur, Transit Campus, Government ITI, Berhampur 760010, Odisha, India*
[3]*School of Earth and Planetary Sciences, National Institute of Science Education and Research, HBNI, Jatni - 752050, India*
[4]*School of Physical Sciences, National Institute of Science Education and Research, HBNI, Jatni, 752050, India*
[5]*Institute of Physics, Jan Kochanowski University, 25-406 Kielce, Poland*

(Received 21 October 2020; revised 23 July 2021; accepted 23 August 2021; published 13 December 2021)

The data on transverse momentum integrated hadron yields in different multiplicity classes of $p + p$ collisions at $\sqrt{s} = 7$ TeV have been analyzed to extract the chemical freeze-out parameters using a thermal model. The chemical freeze-out parameters have been extracted for three different freeze-out schemes: (i) unified freeze-out for all hadrons in complete thermal equilibrium (1CFO), (ii) unified freeze-out for all hadrons with an additional parameter γ_S which accounts for possible out-of-equilibrium production of strange hadrons (1CFO + γ_S), and (iii) separate freeze-out for hadrons with and without strangeness content (2CFO). It has been observed that the 1CFO + γ_S scheme gives the best description of the hadronic yields at midrapidity when multiplicity ($\langle dN_{ch}/d\eta \rangle$) of the collision is less than 10. This indicates that the strangeness is out of equilibrium in most of the multiplicity classes of $p + p$ collisions. All three parameters of this CFO scheme, temperature T, radius R of the fireball, and strangeness suppression factor γ_S increase with the increase of $\langle dN_{ch}/d\eta \rangle$. Furthermore, we have compared applicability of different CFO schemes considering two more colliding systems $p + \mathrm{Pb}$ at $\sqrt{s_{\mathrm{NN}}} = 5.02$ and $\mathrm{Pb} + \mathrm{Pb}$ at $\sqrt{s_{\mathrm{NN}}} = 2.76$ TeV along with $p + p$ collisions at $\sqrt{s} = 7$ TeV. We observe a freeze-out volume (or multiplicity) dependence of CFO schemes regardless of colliding ions. The 1CFO + γ_S, 1CFO, and 2CFO schemes provide the best description of the data when the dimensionless quantity VT^3 approximately satisfies the conditions $VT^3 < 50$, $50 < VT^3 < 100$, and $VT^3 > 100$, respectively, or the corresponding multiplicity satisfies the conditions $\langle dN_{ch}/d\eta \rangle < 30$, $30 < dN_{ch}/d\eta < 60$, and $\langle dN_{ch}/d\eta \rangle > 100$, respectively.

DOI: 10.1103/PhysRevC.104.064905

I. INTRODUCTION

In a high-energy ion collision, a fireball is produced. When the energy density at the core of the fireball is sufficiently high, the quark-gluon plasma (QGP), a deconfined phase of quarks and gluons, is formed. The fireball expands, resulting in a decrease in the temperature. A QGP-to-hadronic phase transition occurs when the temperature drops below the transition temperature. At the initial stage, hadrons interact both elastically and inelastically in the hadronic medium. Inelastic interaction among the hadrons ceases at chemical freeze-out (CFO). At this stage, hadronic yields get fixed and do not change afterwards. The elastic interaction continues until the kinetic freeze-out is reached. Hadrons then stream outwards freely and eventually reach the detector. Experimental data on hadronic yields in ion collisions are traditionally described by the hadron resonance gas (HRG) model. In the most simplified formulation of the HRG model, it is assumed that the CFO of all the hadrons and resonances occurs at the same temperature, baryon chemical potential, and volume of the freeze-out surface. We call this unified CFO scheme 1CFO. This 1CFO HRG model successfully describes the hadron yields in nucleus-nucleus collision across a wide range of center-of-mass energy [1–4]. To describe strange hadrons in elementary collisions like e^+e^-, pp, and $p\bar{p}$ [5–7], an additional parameter γ_s was introduced. The parameter γ_s accounts for the deviation from chemical equilibrium in the strange sector. This CFO scheme is referred to as 1CFO + γ_s. The Pb-Pb collision data at 2.76 TeV indicated a separation of CFO between light and strange quark hadrons [8]. The lattice QCD study also suggested a separate CFO for the strange hadrons [9]. Later, a flavor-dependent sequential freeze-out scheme

*susilkpanda1@gmail.com
†sandeep.chatterjee@fis.agh.edu.pl
‡ajayd@niser.ac.in
§bedanga@niser.ac.in
‖r_paikaray@rediffmail.com
¶subhasis.samant@gmail.com
#ranbir.singh@niser.ac.in

with different freeze-out surfaces for hadrons with zero and nonzero strangeness content was proposed [10]. This CFO scheme is referred to as 2CFO. Thus, despite the phenomenological success of HRG models, it is not clear which CFO scheme is suitable for which data. As a result, the understanding of thermal and chemical equilibration is still an open issue. In Ref. [11] it was shown that the hadron yield for Pb + Pb collisions at $\sqrt{s_{\rm NN}} = 2.76$ TeV [12–15] can be described well with the 2CFO scheme, whereas minimum-bias events of $p+p$ collisions at $\sqrt{s} = 7$ TeV [16–18] prefer 1CFO + γ_S scheme. In this present work, we have done a similar analysis using the newly available data of multiplicity dependence of hadron yield created in $p+p$ collisions at $\sqrt{s} = 7$ TeV [19]. We have also compared multiplicity dependence of different CFO schemes at the CERN Large Hadron Collider (LHC) considering $p+p$ collisions at $\sqrt{s} = 7$ TeV, p + Pb collisions at $\sqrt{s_{\rm NN}} = 5.02$, and Pb + Pb collisions at $\sqrt{s_{\rm NN}} = 2.76$ TeV. Some recent work on multiplicity dependence of freeze-out parameters at the LHC energy can be found in Refs. [20,21].

The paper is arranged in the following way: In Sec. II we discuss different CFO schemes used for this study. The results from the model and data are compared in Sec. III. Finally, we summarize our findings in Sec. IV.

II. DIFFERENT CHEMICAL FREEZE-OUT SCHEMES

A. 1CFO scheme

In the 1CFO scheme, it is assumed that the fireball at the chemical freeze-out is in thermal and chemical equilibrium. The logarithm of the partition function of multicomponent gas of hadrons and resonances in the grand canonical ensemble can be written as

$$\ln Z = \sum_i \ln Z_i, \tag{1}$$

where the sum is over all the species. For ith hadrons

$$\ln Z_i = \pm \frac{V g_i}{2\pi^2} \int_0^\infty p^2 dp \ln\left(1 \pm \exp\left[-(E_i - \mu_i)/T\right]\right), \tag{2}$$

where the upper and lower sign of $\pm$ corresponds to fermions and bosons, respectively. In the last expression, V is the fireball volume, T is the chemical freeze-out temperature. g_i, m_i, μ_i are the degeneracy factor, mass, and chemical potential of the ith hadron, respectively. The chemical potential of the ith hadron can be written as $\mu_i = B_i\mu_B + S_i\mu_S + Q_i\mu_Q$ where B_i, S_i, Q_i are, respectively, the baryon number, strangeness, and electric charge of the hadron. All the chemical potentials are not independent. The μ_S and μ_Q can be extracted by applying the following constraints:

$$\text{Net}S = 0, \tag{3}$$

$$\text{Net}B/\text{Net}Q = r. \tag{4}$$

For $A+A$ collisions, the value of r is $\approx$2.5, while it is 1 for $p+p$ collisions. These constituents come from the conservation of baryon, strangeness, and charge quantum numbers of the colliding ions.

The yield of the ith hadron in the grand canonical ensemble can be written as

$$N_i = T\frac{\partial \ln Z_i}{\partial \mu_i} = \frac{g_i V}{2\pi^2} \sum_{k=1}^{\infty} (\pm)^{k+1} \frac{m_i^2 T}{k} K_2\left(\frac{k m_i}{T}\right) e^{\frac{k\mu_i}{T}}, \tag{5}$$

where K_2 is the modified Bessel function of the second kind. In the last expression, the plus sign is for bosons and the minus sign is for fermions.

Hadronic yields measured by the detectors in experiments include feed-down from heavier hadrons and resonances. Therefore, the total hadronic yield is obtained by including the resonance decay contribution to the above primordial yield

$$N_i^{\rm total} = N_i + \sum_j B.R._{ij} N_j, \tag{6}$$

where $B.R._{ij}$ is the branching ratio for the jth hadron species to ith hadron species.

B. 1CFO + γ_S scheme

In this CFO scheme, incomplete strangeness equilibration is assumed. The hadronic yield in this CFO scheme can be written as [22]

$$N_i = \frac{g_i V}{2\pi^2} \sum_{k=1}^{\infty} (\pm)^{k+1} \frac{m_i^2 T}{k} K_2\left(\frac{k m_i}{T}\right) e^{\frac{k\mu_i}{T}} \gamma_S^{k|S_i|}, \tag{7}$$

where $|S_i|$ is the number of valence strange quarks and antiquarks in the hadron species i. The value $\gamma_S = 1$ corresponds to complete strangeness equilibration. Compared to the 1CFO scheme [Eq. (5)], only the γ_S factor is extra here.

C. 2CFO scheme

The expression of hadronic yield in this CFO scheme is as Eq. (6). However, there are two different sets of parameter for hadrons with and without strangeness content.

Within the GCE ensemble, conservation laws for quantum or particle numbers are enforced on average through the temperature and chemical potentials. It allows fluctuations of conserved averages.

D. Canonical and strangeness canonical ensemble

Apart from the grand canonical ensemble, people have also used other ensembles such as the canonical and strangeness canonical ensembles. In the canonical ensemble (CE), all the charges are exactly conserved [23], whereas in the strangeness canonical ensemble (SCE) [23,24] only strangeness is exactly conserved. Both the CE and SCE are implemented in the THERMUS program [23].

The available experimental data are measured in unit rapidity, so in this work exact conservation is enforced across only a single unit of rapidity.

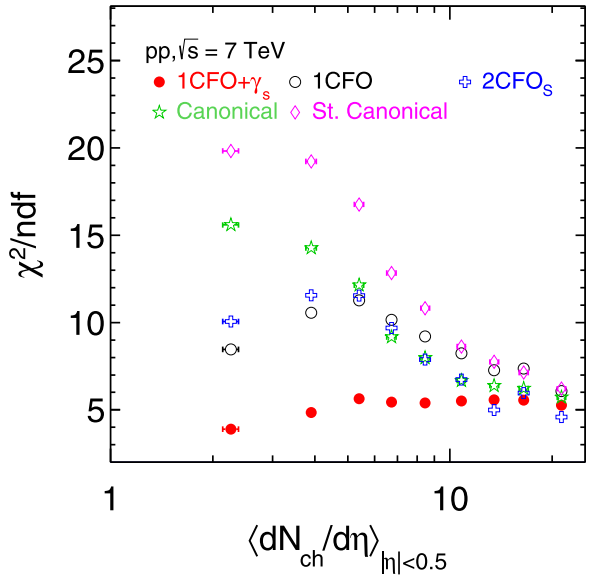

FIG. 1. Variation of χ^2/ndf for the three different freeze-out schemes (1CFO, 1CFO + γ_S, and 2CFO) with the charged particle multiplicity measured at midrapidity in $p+p$ collisions at $\sqrt{s}$ = 7 TeV [19].

III. RESULTS

A. Multiplicity dependence of freeze-out scenarios in $p+p$ collision at LHC

In this work, first we have studied the multiplicity dependence of different CFO schemes in $p+p$ collisions at $\sqrt{s}$ = 7 TeV. For this, we have used data on the p_T-integrated hadron yield in $p+p$ collisions measured at midrapidity at $\sqrt{s}$ = 7 TeV [19]. We have performed our analysis for grand canonical, canonical, and strangeness canonical ensembles using a thermal model called THERMUS [23]. Furthermore, for the grand canonical ensemble, three different freeze-out schemes (1CFO, 1CFO + γ_S, and 2CFO) are considered. For the 1CFO and 1CFO + γ_S schemes, the standard version of THERMUS is used and it extended to include the 2CFO scheme.

To extract the CFO parameters we use available midrapidity yields of the following hadrons: $(\pi^+ + \pi^-)/2$, $(K^+ + K^-)/2$, K^0_s, $(p+\bar{p})/2$, $(K^{*0} + \bar{K}^{*0})/2$, ϕ, $(\Lambda + \bar{\Lambda})/2$, and $(\Xi + \bar{\Xi})/2$. Since an almost equal number of particles and antiparticles are produced at this energy, chemical potentials are taken as zero for all the CFO schemes. Therefore, the parameters to be extracted from the thermal fits in 1CFO are only the fireball volume V and temperature T at the chemical freeze-out. In the 1CFO + γ_S scheme, we have one extra parameter: γ_S. In the 2CFO scheme, different freeze-out volumes and temperatures (V_S, T_S, V_{NS}, and T_{NS}) for the nonstrange and strange hadrons are there. In this CFO scheme, γ_S has no role and hence it is regarded as 1. Therefore, the number of degrees of freedom (ndf = number of data points − number of free parameters) in the 1CFO, 1CFO + γ_S, and 2CFO schemes are 5, 4, and 3, respectively. For the canonical and strangeness canonical ensembles, the free parameters are T, V, and γ_S. In Fig. 1 we compare the goodness of fit in terms of χ^2/ndf of different CFO schemes in different multiplicity classes where the same is defined in terms of charge particle multiplicity. The fitting quality is good for 1CFO + γ_S at lowest $\langle dN_{ch}/d\eta\rangle$ where χ^2/ndf is approximately 3. The χ^2/ndf increases slightly with increasing $\langle dN_{ch}/d\eta\rangle$ and remains within the range 5-6 in other multiplicity classes. For the 1CFO scheme, χ^2/ndf is approximately eight at the lowest $\langle dN_{ch}/d\eta\rangle$ and reaches the highest value (≈12) when $\langle dN_{ch}/d\eta\rangle$ is 3 to 6. The χ^2/ndf then starts decreasing with increasing $\langle dN_{ch}/d\eta\rangle$. Compared to the 1CFO + γ_S scheme, the fitting quality is bad in 1CFO scheme in all the multiplicity classes. Variation of χ^2/ndf with $\langle dN_{ch}/d\eta\rangle$ for 2CFO scheme is almost similar to that of 1CFO. The only difference is that fitting quality becomes comparable to that of 1CFO + γ_S or even better at some multiplicity classes when $\langle dN_{ch}/d\eta\rangle > 10$.

1. Results of canonical ensemble

Along with the results of the grand canonical ensemble, we have also shown the quality of fitting in the canonical ensemble (CE) in Fig. 1. At the lowest $\langle dN_{ch}/d\eta\rangle$, χ^2/ndf for CE is 15.59 which is much larger than that of three CFO schemes in grand canonical ensembles. It then decreases with increase of $\langle dN_{ch}/d\eta\rangle$. The χ^2/ndf for CE is greater than that of the 1CFO + γ_s scheme in the whole range of multiplicities shown in this figure. Another significant difference is that the extracted chemical freeze-out temperature in the CE is too large compared with those of the GCE and QCD crossover temperature, which is around 155 MeV. At the lowest multiplicity, T is around 194 MeV. The temperature decreases with increasing multiplicity and reaches 173 MeV at the highest multiplicity. We have observed that the ϕ meson is responsible for large χ^2/ndf in the CE. If we exclude ϕ in the fitting, χ^2/ndf in the lowest multiplicity class goes down from 15.59 to 2.54. We compared our result for the CE with previous work in Ref. [20]. It has been shown in Ref. [20] that the CE gives the best result in the low-multiplicity region, which seems to contradict our result. However, this is not the case because different sets of particles are used in both analyses. Particularly in Ref. [20], K_s, K^*, and ϕ are excluded from the fitting. Another difference is the inclusion of Ω which is not there in our fitting. Already we have discussed the issue with the ϕ meson. Furthermore, we checked the effect on our results by excluding K_s, K^*, and ϕ. If we remove only K^* and ϕ, χ^2/ndf at lowest $\langle dN_{ch}/d\eta\rangle$ goes down from 15.59 to 1.28. By excluding K^*, ϕ, and K_s, χ^2/ndf becomes even better (0.9). The corresponding chemical freeze-out temperatures in these two cases are 201 and 202 MeV, respectively. So, although there is an improvement of χ^2/ndf, the chemical freeze-out temperature is still absurd. This indicates that the CE is not suitable for the LHC energy. In the presence of the ϕ meson, a large freeze-out temperature in the CE was also reported in Ref. [21]. The reason for the failure of CE is probably because the accepted rapidity region is much smaller than the total rapidity. The system is more like a grand canonical rather than canonical ensemble. There is no reason that the baryon, strangeness, and electric charge will be exactly conserved at one unit of rapidity region. It is argued in Ref. [21] that, for the exact conservation of these charges, several units of rapidity interval around the midrapidity are needed rather than a single

TABLE I. The chemical freeze-out parameters in the 1CFO, 1CFO + γ_s, and 2CFO schemes in $p+p$ collisions at $\sqrt{s} = 7$ TeV for different multiplicity classes.

	1CFO (1CFO + γ_s)			2CFO			
				Strange		Nonstrange	
Centrality (%)	T (MeV)	R (fm)	γ_s	T_S (MeV)	R_S (fm)	T_{NS} (MeV)	R_{NS} (fm)
0–1	162 ± 3 (164 ± 3)	2.29 ± 0.10 (2.30 ± 0.11)	0.89 ± 0.03	167 ± 3	2.06 ± 0.10	145 ± 4	3.16 ± 0.20
1–5	160 ± 3 (163 ± 3)	2.15 ± 0.09 (2.16 ± 0.10)	0.86 ± 0.03	165 ± 3	1.93 ± 0.09	145 ± 3	2.90 ± 0.15
5–10	161 ± 3 (163 ± 3)	1.99 ± 0.09 (2.01 ± 0.09)	0.86 ± 0.03	166 ± 3	1.78 ± 0.09	145 ± 3	2.71 ± 0.13
10–20	159 ± 3 (162 ± 3)	1.89 ± 0.08 (1.91 ± 0.08)	0.84 ± 0.03	164 ± 3	1.70 ± 0.09	146 ± 3	2.52 ± 0.14
20–30	158 ± 3 (161 ± 3)	1.77 ± 0.08 (1.80 ± 0.08)	0.82 ± 0.03	163 ± 3	1.60 ± 0.08	146 ± 3	2.34 ± 0.13
30–40	157 ± 3 (160 ± 3)	1.69 ± 0.07 (1.71 ± 0.08)	0.80 ± 0.03	161 ± 3	1.52 ± 0.08	146 ± 3	2.18 ± 0.12
40–50	156 ± 3 (159 ± 3)	1.58 ± 0.07 (1.62 ± 0.07)	0.78 ± 0.03	160 ± 3	1.43 ± 0.07	145 ± 3	2.05 ± 0.12
50–70	153 ± 3 (157 ± 3)	1.47 ± 0.07 (1.51 ± 0.07)	0.76 ± 0.03	157 ± 3	1.35 ± 0.07	144 ± 4	1.88 ± 0.12
70–100	148 ± 3 (152 ± 3)	1.33 ± 0.07 (1.38 ± 0.07)	0.72 ± 0.04	149 ± 3	1.27 ± 0.07	140 ± 4	1.69 ± 0.13

unit. Because of these problems in the CE, we do not consider the CE in the rest of the paper.

2. Results of strangeness canonical ensemble

In Fig. 1, the worst fit is observed in the case of the SCE. χ^2/ndf is ≈20 at the lowest $\langle dN_{ch}/d\eta \rangle$. Similar to the CE, χ^2/ndf for the SCE decreases with increasing $\langle dN_{ch}/d\eta \rangle$. χ^2/ndf for the SCE is always larger than that of the 1CFO + γ_s scheme. Again a relatively better χ^2/ndf is shown in Ref. [20] but with the cost of giving up K_s, K^*, and ϕ in the fit. Since χ^2/ndf in Fig. 1 is bad in the SCE, we will not consider this CFO scheme in the rest of the paper.

Overall from Fig. 1, we can say that, except a few multiplicity classes, the 1CFO + γ_S scheme is better compared with other CFO schemes.

3. Extracted chemical freeze-out parameters and comparison between data and model

The extracted chemical freeze-out parameters in different multiplicity classes are listed in Table I, where, instead of $\langle dN_{ch}/d\eta \rangle$, the percent centrality is mentioned [19]. Note that $\langle dN_{ch}/d\eta \rangle$ decreases as the percent centrality increases. The $\langle dN_{ch}/d\eta \rangle$ dependence of the chemical freeze-out temperature, the radius of the fireball, and the strangeness suppression factor in three different CFO schemes are shown in Fig. 2. At the lowest value of $\langle dN_{ch}/d\eta \rangle$, the temperature is around 152 MeV for the 1CFO + γ_S scheme. The temperature gradually increases with the increase of $\langle dN_{ch}/d\eta \rangle$ and reaches around 164 MeV at the highest $\langle dN_{ch}/d\eta \rangle$. Similar temperatures are obtained for the 1CFO scheme as well. On the other hand, for the 2CFO scheme, a clear separation of freeze-out temperature of the nonstrange and strange hadrons is observed and the separation increases with increasing $\langle dN_{ch}/d\eta \rangle$. The multiplicity dependence of the freeze-out temperature of strange hadrons in the 2CFO scheme is similar to the 1CFO and 1CFO + γ_S schemes. However, no such multiplicity dependence of freeze-out temperature is observed for the nonstrange hadrons in this CFO scheme. Not only that, the freeze-out temperature of nonstrange hadrons, which lies around 145 MeV, is significantly (5–20 MeV) lower compared with that of strange hadrons, which suggests that the strange hadrons freeze earlier compared with nonstrange hadrons. Compared to different CFO schemes in the grand canonical ensemble, the larger temperature is observed for the canonical ensemble in all $\langle dN_{ch}/d\eta \rangle$. Although it is not shown still we would like to mention here that the extracted temperature at lowest $\langle dN_{ch}/d\eta \rangle$ for CE is around 195 MeV, which is very large compared with other CFO schemes and therefore seems unrealistic.

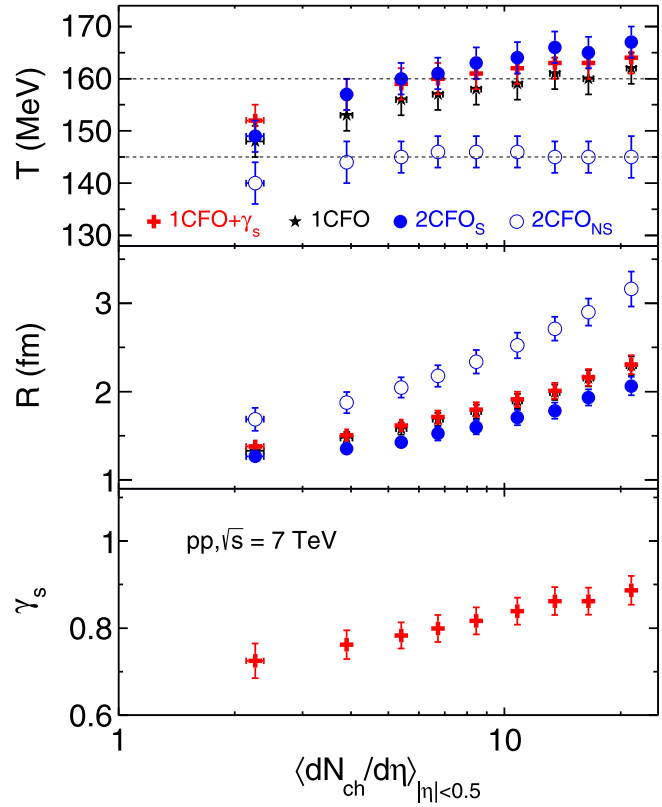

FIG. 2. The multiplicity dependence of chemical freeze-out parameters (temperature T, radius R, and strangeness nonequilibrium factor γ_S) obtained in three different freeze-out schemes.

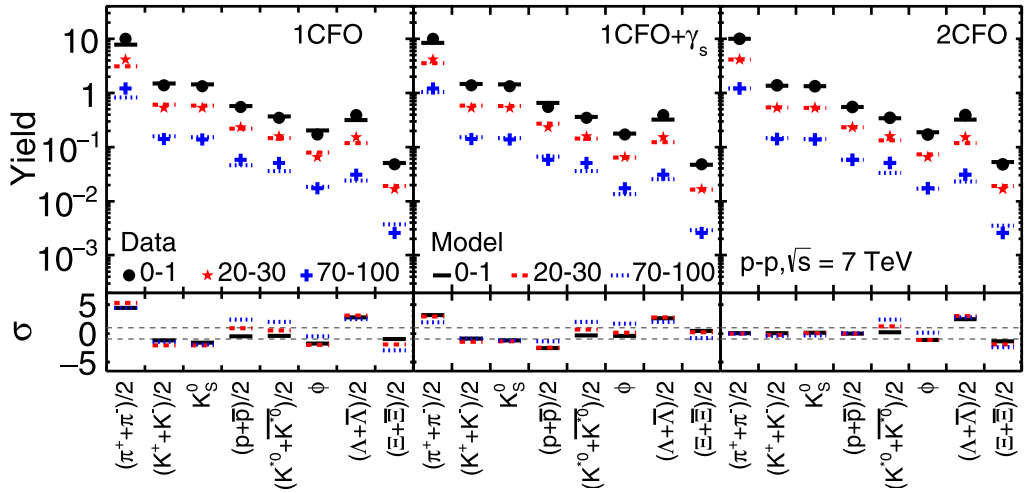

FIG. 3. Comparison between data [19] and model [23] for $p+p$ collisions at $\sqrt{s} = 7$ TeV in three different freeze-out schemes: 1CFO (left column), 1CFO + γ_S (middle column), and 2CFO (right column). The deviations of the data from the model [Eq. (8)] for each freeze-out scheme are also shown.

The middle panel of Fig. 2 shows the multiplicity dependence of the fireball radius at freeze-out. As expected, R increases with increasing $\langle dN_{ch}/d\eta \rangle$ in all CFO schemes in the grand canonical ensemble. Similar to the temperature, freeze-out radii are also close to each other in the 1CFO and 1CFO + γ_S schemes. In these two CFO schemes, R is around 1.3 fm at the lower $\langle dN_{ch}/d\eta \rangle$ and reaches up to ≈2.3 fm at the highest $\langle dN_{ch}/d\eta \rangle$. Again in the 2CFO scheme, two separate freeze-out radii are observed for strange and nonstrange hadrons. The extracted size of the fireball for nonstrange hadrons is larger than that of strange hadrons in all multiplicity classes.

The multiplicity dependence of the strangeness suppression factor is shown in the lower panel of Fig. 2. At the lowest $\langle dN_{ch}/d\eta \rangle$, γ_S is around 0.72, which is far away from the equilibrium value of 1. With the increase of $\langle dN_{ch}/d\eta \rangle$, γ_S gradually increases towards its equilibrium value and reaches up to 0.89 at the highest $\langle dN_{ch}/d\eta \rangle$, which indicates that full strangeness equilibration is not achieved at lower values of $\langle dN_{ch}/d\eta \rangle$. However, it is moving towards the equilibrium when $\langle dN_{ch}/d\eta \rangle$ is relatively larger. Therefore, it is expected that the CFO scheme which deals with the nonequilibrium situation of the strange hadron is the best suited when $\langle dN_{ch}/d\eta \rangle$ is small. For this reason, in the previous figure (Fig. 1), better fitting quality (i.e., lower χ^2/ndf) at lower $\langle dN_{ch}/d\eta \rangle$ was observed in the 1CFO + γ_S scheme compared with other 1CFO and 2CFO schemes, where full equilibration was assumed.

We have observed that the extracted freeze-out temperature and γ_s in the 1CFO + γ_s scheme in this present work is in good agreement with those of Ref. [20] despite having the difference in the fitted particle list mentioned previously.

Now we will discuss the comparison between experimental data of hadrons and model estimation. For the rest of the paper, we consider CFO schemes in grand canonical ensemble only since in Fig. 1 we have already seen that the fitting quality is much better in the grand canonical ensemble combined with the CE or SCE. In the upper panels of Fig. 3, we compare experimentally measured hadronic yields with the best-fitted model calculation in the three CFO schemes: 1CFO (left column), 1CFO + γ_S (middle column), and 2CFO (right column). For illustration purposes, we choose only three multiplicity bins: 0%–1%, 20%–30% and 70%–100%. Experimental data are indicated by solid points while a line is used to show the model estimation. The lower panel of this figure shows the deviation which is defined as

$$\sigma = \frac{\text{Data} - \text{Model}}{\text{Error of data}}. \tag{8}$$

Horizontal lines at ±1 are drawn to indicate ±1σ deviation. Deviations are less than 3σ for all the hadrons except pions in the 1CFO scheme. In the 1CFO + γ_S scheme, significant improvement is observed, particularly in the 70%–100% centrality class where the modulus of deviation is less than 2σ for all the hadrons including pion. On the other hand, for all the centrality classes, descriptions of π, K, K_s^0, and p are very good (the modulus of the deviation is less than 1σ) in the 2CFO scheme. However, it is not good for strange hadrons such as $K^\star$, Λ, and Ξ in 70%–100% centrality class. These hadrons are described better in the 1CFO + γ_S scheme. Note that a separate freeze-out surface is used for the hadrons containing the strange quark in the 2CFO scheme; still, its performance is not better than the 1CFO + γ_S scheme. The description of both nonstrange and strange hadrons in 70%–100% centrality is better in the 1CFO + γ_S scheme compared with the other two CFO schemes. The χ^2/ndf is also smaller in the 1CFO + γ_S scheme (see Fig. 1). Therefore, we can say that 1CFO + γ_S is the most appropriate freeze-out scenario for 70%–100% centrality class. The same is true for the 20%–30% multiplicity classes as well. As we move toward higher multiplicity class, improvement is observed in the 2CFO scheme. In the 0%–1% multiplicity class, the description of π, K, K_s^0, and p is better in 2CFO scheme compared with the 1CFO and 1CFO + γ_S schemes. As a result, χ^2/ndf is slightly small in the case of the 2CFO scheme compared with the other two CFO schemes in this multiplicity class.

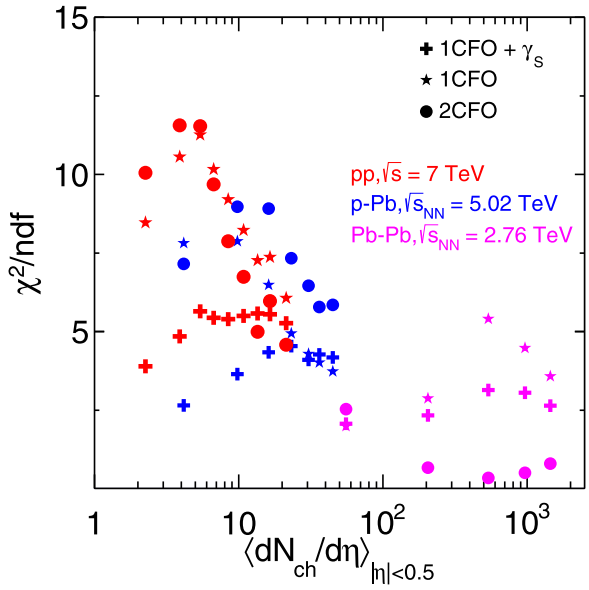

FIG. 4. χ^2/ndf in three different CFO schemes in the grand canonical ensemble as a function of average charged-particle multiplicity in $p+p$ collisions at $\sqrt{s} = 7$ TeV and compared with the same in $p+$Pb and Pb + Pb collisions at $\sqrt{s_{\rm NN}} = 5.02$ [25–27] and 2.76 TeV [12–15], respectively.

B. Comparison of different freeze-out scenarios at LHC

We now present a broader picture of the multiplicity dependence of freeze-out scenarios at the LHC. Here we consider collision systems $p+$Pb and Pb + Pb along with $p+p$. In Fig. 4 we show the multiplicity dependence of least χ^2/ndf. Here we have taken some data from the previously published results of $p+$Pb and Pb + Pb collisions at $\sqrt{s_{\rm NN}} = 5.02$ and 2.76 TeV, respectively [11], combined with the present results of $p+p$ collision at $\sqrt{s} = 7$ TeV. The left panel shows χ^2/ndf in three different CFO schemes in the grand canonical ensemble as a function of $\langle dN_{ch}/d\eta \rangle$. Different marker styles are used for different CFO schemes, while different color is used for different collision systems. For the $p+p$ collision, the result is already discussed in Fig. 1. For $p+$Pb collisions, the lowest χ^2/ndf is observed in the 1CFO + γ_s scheme when $\langle dN_{ch}/d\eta \rangle < 30$. Above this, the 1CFO scheme performs better. For Pb + Pb collision, 2CFO gives the best result when $\langle dN_{ch}/d\eta \rangle > 100$. Below this multiplicity, 1CFO performs well. The variation of $\langle dN_{ch}/d\eta \rangle$ at the LHC is more than three orders of magnitude. Based on the applicability of different CFO schemes, we can divide the whole range of $\langle dN_{ch}/d\eta \rangle$ into three regions: low ($\langle dN_{ch}/d\eta \rangle < 30$), intermediate ($30 < \langle dN_{ch}/d\eta \rangle < 60$), and high ($\langle dN_{ch}/d\eta \rangle > 100$) multiplicities. Note that, presently, no data are available in the range $60 < \langle dN_{ch}/d\eta \rangle < 100$. All $p+p$ collisions and $p+$Pb collisions where $\langle dN_{ch}/d\eta \rangle < 30$ are best described by the 1CFO + γ_S scheme, which is indicated by plus markers. It indicates that strange hadrons containing strange quarks are out of equilibrium when $\langle dN_{ch}/d\eta \rangle < 30$. In small systems, the fireball lifetime is expected to be small. As a result, interaction among constituents is not sufficient to achieve equilibration. The equilibrium CFO schemes are good only if

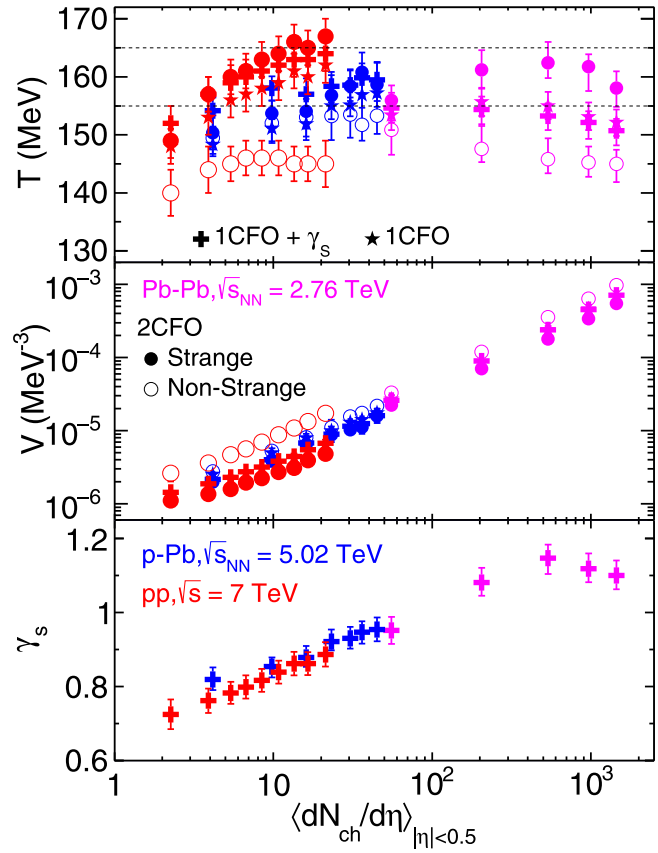

FIG. 5. Extracted freeze-out parameters in three different CFO schemes in grand canonical ensemble as a function $\langle dN_{ch}/d\eta \rangle$ considering three different collision systems: $p+p$ at $\sqrt{s} = 7$ TeV, $p+$Pb at $\sqrt{s_{\rm NN}} = 5.02$, and Pb + Pb collisions at $\sqrt{s_{\rm NN}} = 2.76$ TeV.

$\langle dN_{ch}/d\eta \rangle$ is approximately greater than 30. For the intermediate range of multiplicity ($30 < \langle dN_{ch}/d\eta \rangle < 60$), the 1CFO scheme has the least χ^2/ndf, which is shown by star markers. High-multiplicity $p+$Pb and low-multiplicity Pb + Pb collisions fall in this category. The Pb + Pb collisions with $\langle dN_{ch}/d\eta \rangle > 100$ can be best described by the 2CFO scheme, which is shown by circular markers.

In the three panels of Fig. 5 we show the multiplicity dependence of the freeze-out temperature (top panel), the volume of the fireball (middle panel), and the γ_S (bottom panel) at the LHC using the three different CFO schemes in the grand canonical ensemble. Freeze-out parameters of $p+$Pb and Pb + Pb collisions at $\sqrt{s_{\rm NN}} = 5.02$ and 2.76 TeV, respectively, are taken from Ref. [11]. We have already discussed the results of $p+p$ collision at $\sqrt{s} = 7$ TeV in Fig. 2. One can see that, compared with $p+p$ collisions, the freeze-out temperatures in different CFO schemes for $p+$Pb collisions are much closer to each other and lie around 155 MeV. Furthermore, no multiplicity dependence of temperature is observed in the case of $p+$Pb collisions. On the other hand, for Pb + Pb collisions, the freeze-out temperature is around 155 MeV for the 1CFO and 1CFO + γ_s schemes, while for the 2CFO scheme, the temperature is slightly higher than 155 MeV for strange hadrons and slightly lower for nonstrange hadrons. Here also, no significant multiplicity dependence is observed.

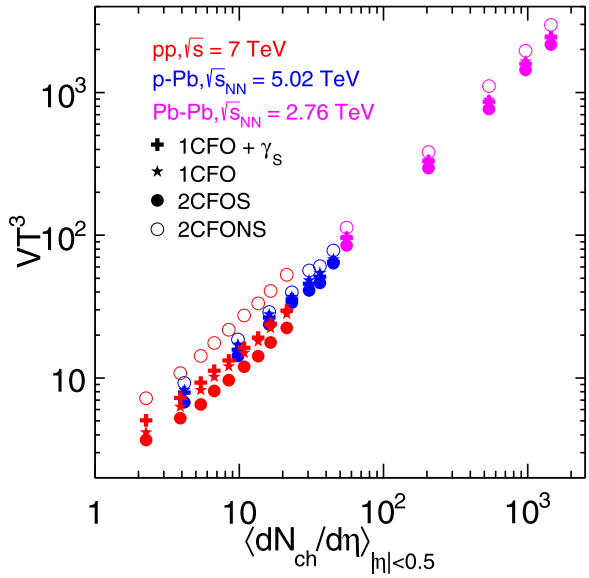

FIG. 6. Product of extracted volume and temperature cube as a function of average charged-particle multiplicity in $p+p$ collisions at $\sqrt{s}=7$ TeV and compared with the same in $p+$Pb and Pb + Pb collisions at $\sqrt{s_{\rm NN}}=5.02$ and 2.76 TeV [11], respectively, for the best freeze-out scheme.

Now let us discuss the best-fit results of freeze-out temperature. For the low and intermediate regions of multiplicity ($\langle dN_{ch}/d\eta\rangle < 60$), the best-fit (for which χ^2/ndf is a minimum) freeze-out temperature lies in the range 155–165 MeV. In the high-multiplicity region ($\langle dN_{ch}/d\eta\rangle > 100$), the freeze-out temperature of the hadrons containing strange quarks also lies within this range. However, for nonstrange hadrons, the temperature is approximately 15 MeV less. It means that nonstrange hadrons freeze-out later than strange hadrons when $\langle dN_{ch}/d\eta\rangle > 100$. The volume of the fireball at the freeze-out increases almost linearly with the multiplicity. Volumes for 1CFO and 1CFO + γ_s are almost the same in all $\langle dN_{ch}/d\eta\rangle$. In the 2CFO scheme, the freeze-out volumes of strange and nonstrange are different and the volume is larger for the nonstrange hadrons since they freeze-out later. Overall we observe a smooth variation of volume from one collision system to another. With the increase of multiplicity, γ_S increases towards unity, and for Pb + Pb collisions γ_S is greater than one. Values of γ_S for different data sets lie in a line. Here also we observe a smooth variation from one system to another. Note the best-fit result suggests that γ_S is only needed for the low-multiplicity events. Above $\langle dN_{ch}/d\eta\rangle \approx 30$ an equilibration CFO schemes, either 1CFO or 2CFO can be used.

Instead of multiplicity, we can also separate three zones in terms of the dimensionless quality VT^3 since it is proportional to $\langle dN_{ch}/d\eta\rangle$, and this is presented in Fig. 6. This figure shows that the 1CFO + γ_S scheme is the best for the small freeze-out system where $VT^3 < 50$. For intermediate system size, where $50 < VT^3 < 100$, 1CFO performs well, whereas, for a large system where $VT^3 > 100$, the 2CFO scheme is more suitable. We observe that the best-fit value of VT^3 increases almost linearly with the multiplicity even though a different CFO scheme is suitable for the different zone of multiplicity. Furthermore, Fig. 6 shows that our treatment in the grand canonical ensemble is justified since $VT^3 > 1$ in all multiplicity classes for all collision systems [24].

IV. SUMMARY

We have studied the transverse momentum integrated hadron yields in different multiplicity classes of $p+p$ collisions at $\sqrt{s}=7$ TeV using a thermal model (THERMUS) and extracted the CFO parameters. Analysis has been done for different CFO schemes, i.e., 1CFO, 1CFO + γ_S, and 2CFO in the grand canonical ensemble. The analysis is also done for the canonical and strangeness canonical ensemble. Charge conservation is enforced across only a single unit of rapidity within which experimental data are available. Within this limitation it has been observed that, for most of the multiplicity classes, the 1CFO + γ_S scheme best describes the data. The value of γ_S varies between 0.72 and 0.89, which indicates that hadrons containing strange quarks are out of equilibrium at the freeze-out in all multiplicity classes. With the increase of multiplicity the chemical freeze-out temperature increases from 152 to 164 MeV. The fireball size also increases with increases of multiplicity and the radius varies from 1.38 to 2.3 fm.

We have also tried to understand the applicability of different CFO schemes at the LHC considering two other collision systems: $p+$Pb and Pb + Pb, at $\sqrt{s_{\rm NN}}=5.02$ and 2.76 TeV, respectively. We observed a multiplicity (or freeze-out volume) dependence of CFO schemes instead of colliding ion and energy dependence. The 1CFO + γ_S scheme is suitable to describe the hadronic yield when multiplicity is less than 30, whereas 2CFO performs the best when multiplicity is larger than 100. In the intermediate region $30 < dN_{ch}/d\eta < 601$, the CFO gives the best description of the data. The same conclusion can be drawn in terms of freeze-out volume as well. The 1CFO + γ_S, 1CFO, and 2CFO schemes best description of the data when the dimensionless quantity VT^3 satisfies the conditions $VT^3 < 50$, $50 < VT^3 < 100$, and $VT^3 > 100$, respectively.

ACKNOWLEDGMENTS

A.K.D. and R.S. acknowledge the support of the XIIth plan Project no. 12-R&D-NIS-5.11-0300 of the Government of India. B.M. acknowledges financial support from J.C. Bose National Fellowship of DST, Government of India. S.S. acknowledges financial support from the Polish National Agency for Academic Exchange through an Ulam Scholarship with agreement no. PPN/ULM/2019/1/00093/U/00001.

[1] P. Braun-Munzinger, J. Stachel, J. P. Wessels, and N. Xu, Phys. Lett. B **365**, 1 (1996).

[2] G. D. Yen and M. I. Gorenstein, Phys. Rev. C **59**, 2788 (1999).

[3] P. Braun-Munzinger, I. Heppe, and J. Stachel, Phys. Lett. B **465**, 15 (1999).
[4] A. Andronic, P. Braun-Munzinger, and J. Stachel, Nucl. Phys. A **772**, 167 (2006).
[5] F. Becattini, Z. Phys. C: Part. Fields **69**, 485 (1996).
[6] F. Becattini, A. Giovannini, and S. Lupia, Z. Phys. C: Part. Fields **72**, 491 (1996).
[7] F. Becattini and U. W. Heinz, Z. Phys. C: Part. Fields **76**, 269 (1997); **76**, 578 (1997).
[8] B. Abelev *et al.* (ALICE Collaboration), Phys. Rev. Lett. **109**, 252301 (2012).
[9] R. Bellwied, S. Borsanyi, Z. Fodor, S. D. Katz, and C. Ratti, Phys. Rev. Lett. **111**, 202302 (2013).
[10] S. Chatterjee, R. M. Godbole, and S. Gupta, Phys. Lett. B **727**, 554 (2013).
[11] S. Chatterjee, A. K. Dash, and B. Mohanty, J. Phys. G **44**, 105106 (2017).
[12] B. Abelev *et al.* (ALICE Collaboration), Phys. Rev. C **88**, 044910 (2013).
[13] B. B. Abelev *et al.* (ALICE Collaboration), Phys. Rev. Lett. **111**, 222301 (2013).
[14] B. B. Abelev *et al.* (ALICE Collaboration), Phys. Lett. B **728**, 216 (2014); **734**, 409 (2014).
[15] B. B. Abelev *et al.* (ALICE Collaboration), Phys. Rev. C **91**, 024609 (2015).
[16] B. Abelev *et al.* (ALICE Collaboration), Eur. Phys. J. C **72**, 2183 (2012).
[17] B. Abelev *et al.* (ALICE Collaboration), Phys. Lett. B **712**, 309 (2012).
[18] J. Adam *et al.* (ALICE Collaboration), Eur. Phys. J. C **75**, 226 (2015).
[19] S. Acharya *et al.* (ALICE Collaboration), Phys. Rev. C **99**, 024906 (2019).
[20] N. Sharma, J. Cleymans, B. Hippolyte, and M. Paradza, Phys. Rev. C **99**, 044914 (2019).
[21] V. Vovchenko, B. Dönigus, and H. Stoecker, Phys. Rev. C **100**, 054906 (2019).
[22] S. Das, D. Mishra, S. Chatterjee, and B. Mohanty, Phys. Rev. C **95**, 014912 (2017).
[23] S. Wheaton and J. Cleymans, Comput. Phys. Commun. **180**, 84 (2009).
[24] I. Kraus, J. Cleymans, H. Oeschler, and K. Redlich, Phys. Rev. C **79**, 014901 (2009).
[25] B. B. Abelev *et al.* (ALICE Collaboration), Phys. Lett. B **728**, 25 (2014).
[26] J. Adam *et al.* (ALICE Collaboration), Phys. Lett. B **758**, 389 (2016).
[27] J. Adam *et al.* (ALICE Collaboration), Eur. Phys. J. C **76**, 245 (2016).